ACS Medicinal Chemistry Letters

pubs.acs.org/acsmedchemlett Letter

Structure–Activity and Brain Kinetics Relationships of ^{18}F-Labeled Benzimidazopyridine Derivatives as Tau PET Tracers

Hiroyuki Watanabe,* Yuta Tarumizu, Sho Kaide, Yoichi Shimizu, Shimpei Iikuni, Yuji Nakamoto, and Masahiro Ono*

Cite This: *ACS Med. Chem. Lett.* 2021, 12, 262–266 Read Online

ACCESS | Metrics & More | Article Recommendations | Supporting Information

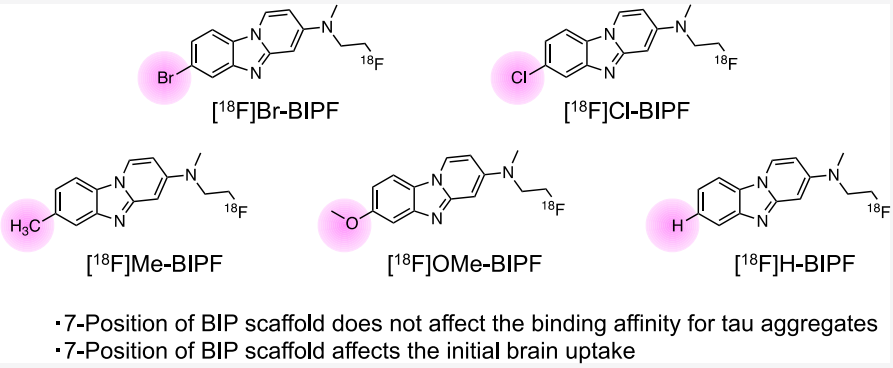

ABSTRACT: Noninvasive imaging of tau aggregates with a positron emission tomography (PET) tracer is useful for the diagnosis and staging of Alzheimer's disease (AD). Recently, we found that benzimidazopyridine (BIP) is an attractive scaffold for developing PET and single photon computed emission tomography tracers targeting tau aggregates. In this study, we designed and synthesized five novel ^{18}F-labeled compounds with various substituted groups or atoms at the 7-position of the BIP scaffold. In *in vitro* autoradiographic studies, all ^{18}F-labeled BIP derivatives selectively bound to tau aggregates deposited in AD brain sections. On the other hand, the initial brain uptake of these compounds was affected by the type of substituted group or halogen atom introduced into the 7-position of the BIP scaffold. Among these compounds, [^{18}F]Me-BIPF showed the highest brain uptake (6.79% ID/g at 2 min postinjection) and 2 min/60 min ratio (3.59). These results suggest that appropriate introduction of the substituted group or atom into the 7-position of the BIP scaffold may be effective for developing useful tau PET tracers.

KEYWORDS: *Alzheimer's disease, tau imaging, PET, ^{18}F*

Misfolded protein aggregates in the brain are characteristic of various neurodegenerative disorders, such as Alzheimer's disease (AD), Parkinson's disease, and amyotrophic lateral sclerosis.[1,2] AD is a progressive degenerative brain disease and the most common form of dementia in the elderly, but diagnostic and treatment methods have not been established.[3] The deposition of neurofibrillary tangles, which are composed of hyperphosphorylated tau protein aggregates, is one of the major hallmarks in the AD brain.[2,4] Since the spreading of neurofibrillary tangles closely corresponds to the level of cognitive impairment in AD, the detection of tau aggregates *in vivo* is valuable for the diagnosis and monitoring the progression of AD. Several positron emission tomography (PET) tracers targeting tau aggregates have been developed and tested in humans. First generation ([^{18}F]AV-1451 (flortaucipir or T807), [^{18}F]THK-5351, and [^{11}C]PBB3) and second generation tau PET tracers such as [^{18}F]MK-6240, [^{18}F]RO-948, [^{18}F]PI-2620, and [^{18}F]GTP1 have been developed and tested in humans.[5−12] The first generation tracers have some problems including off-target binding, but [^{18}F]AV-1451 is the most commonly used in clinical studies. Many clinical studies using second generation tracers are ongoing. The results of these clinical studies have indicated their utility as a tool for the diagnosis and clinical management of AD.

We recently reported that the benzimidazopyridine (BIP) scaffold is useful for the development of tau tracers (Figure 1).[13−15] First, we found that [^{125}I]BIP-NMe$_2$ selectively bound to tau aggregates in AD brain sections and displayed favorable brain kinetics in the normal mouse.[13] Next, we performed a structure–activity brain kinetics relationship study involving

Received: December 7, 2020
Accepted: January 4, 2021
Published: January 11, 2021

https://dx.doi.org/10.1021/acsmedchemlett.0c00641
ACS Med. Chem. Lett. 2021, 12, 262–266

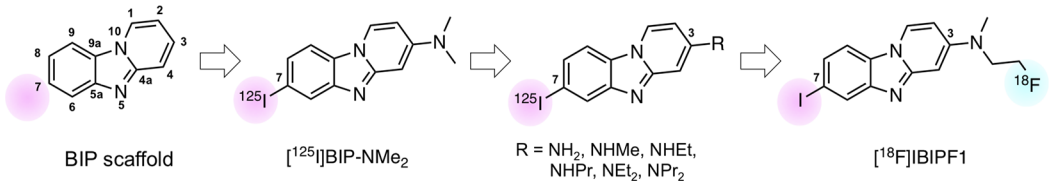

Figure 1. Chemical structures of BIP derivatives tested in the previous study.

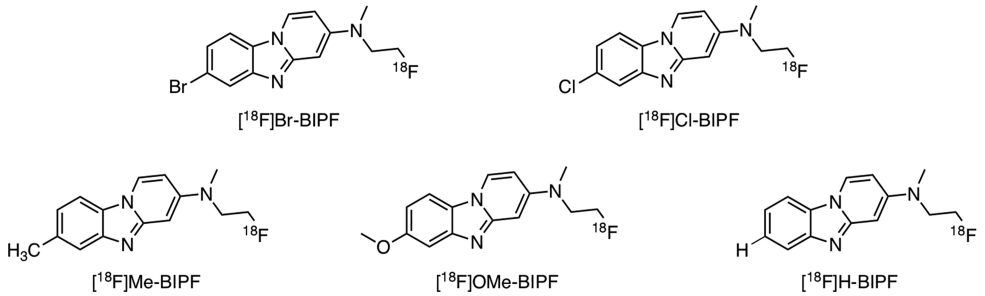

Figure 2. Chemical structures of ^{18}F-labeled BIP derivatives developed in this study.

Scheme 1. Synthetic Route of BIP Derivatives and Precursors for Radiosynthesis

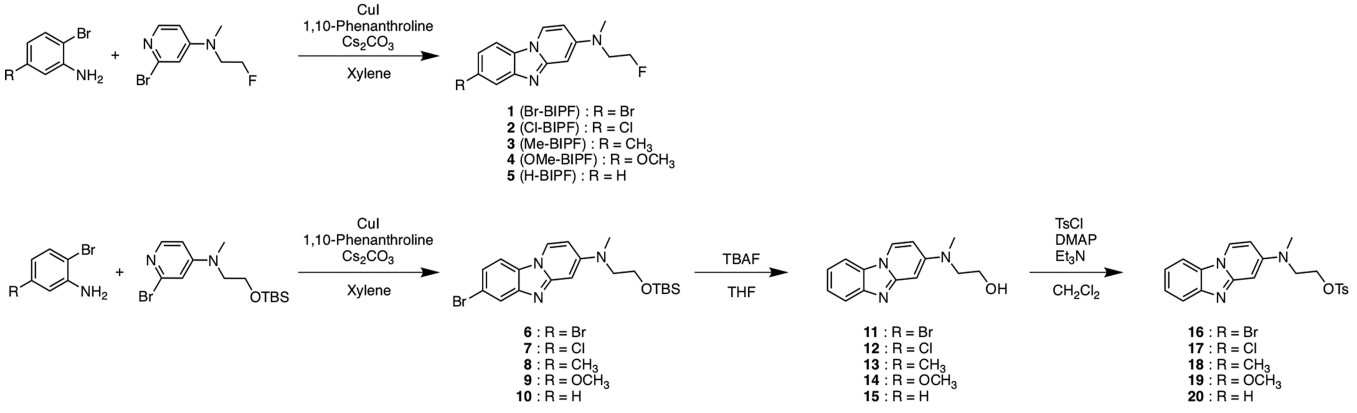

Scheme 2. Synthetic Route of ^{18}F-Labeled BIP Derivatives

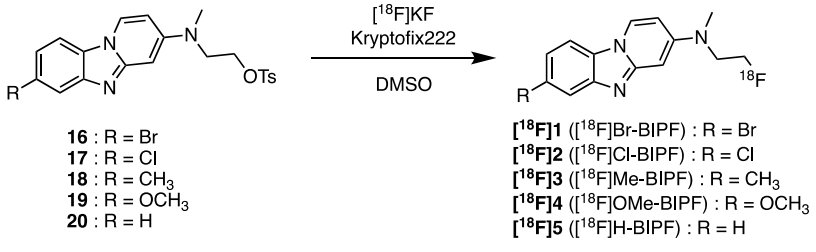

the introduction of various types of alkylamino groups into the 3-position of the BIP scaffold.[14] The results of this study indicated that the change in the substituted group at the 3-position of the BIP scaffold affects the binding affinity for tau aggregates and brain uptake in the murine brain. Based on the findings, we recently developed two PET tracers ([^{18}F]IBIPF1 and [^{18}F]IBIPF2) based on the BIP scaffold.[15] The results of this study suggested that [^{18}F]IBIPF1 showed potential as a tau PET tracer, and further modifications may lead to the development of more useful tracers for the detection of tau aggregates in the brain.

We have developed many BIP derivatives, containing radioiodine at the 7-position of the BIP scaffold, as radioiodinated tau SPECT tracers (Figure 1).[13,14] However, the introduction of an iodine atom into the BIP scaffold is not necessary for the development of ^{18}F-labeled tau PET tracers. Therefore, we planned to evaluate the effect of the substituted group at the 7-position of the BIP scaffold on the affinity for tau aggregates and brain kinetics in the mouse. First, we choose halogen atoms (bromine and chloride), which are in the same family as the iodine atom. In addition, since tau SPECT tracers with methyl and methoxy groups and no substituted group at the 3-position of BIP derivatives were previously evaluated, we newly designed and synthesized five ^{18}F-labeled compounds with a halogen atom ([^{18}F]Br-BIPF and [^{18}F]Cl-BIPF), methyl group ([^{18}F]Me-BIPF), methoxy group ([^{18}F]OMe-BIPF), or no substituted group ([^{18}F]H-BIPF) at the 7-position of the

https://dx.doi.org/10.1021/acsmedchemlett.0c00641
ACS Med. Chem. Lett. 2021, 12, 262−266

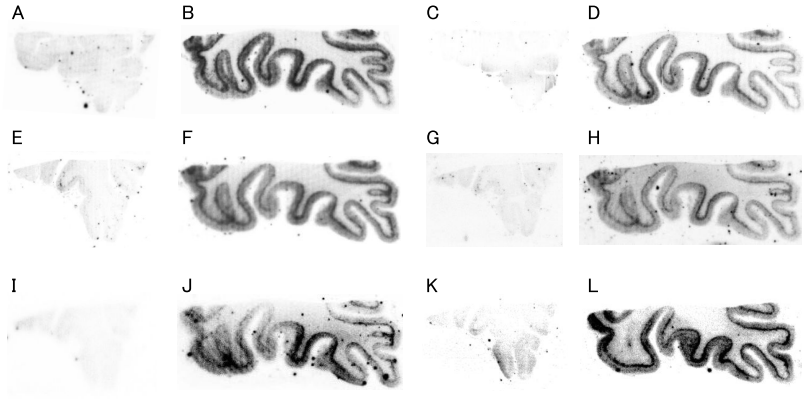

Figure 3. Comparison of *in vitro* autoradiography of [^{18}F]Br-BIPF (A and B), [^{18}F]Cl-BIPF (C and D), [^{18}F]Me-BIPF (E and F), [^{18}F]OMe-BIPF (G and H), [^{18}F]H-BIPF (I and J), and [^{18}F]RO-948 (K and L) in brain sections from AD patients. Panels (A), (C), (E), (G), (I), and (K) show results in Aβ(+)/tau(−) brain sections. Panels (B), (D), (F), (H), (J), and (L) show results in Aβ(+)/tau(+) brain sections.

BIP scaffold (Figure 2) and evaluated their *in vitro* and *in vivo* characteristics as tau PET tracers.

The synthetic route of novel BIP derivatives is shown in Scheme 1. 2-Bromopyridine derivatives were synthesized according to a previously reported method.[15] The BIP scaffold (**1**−**10**) was also formed by a method previously reported in yields of 5−45%.[13] After the removal of *tert*-butyldimethylsilyl (TBS) groups of **6**−**10**, the hydroxyl groups of **11**−**15** were converted into tosylates by reacting *p*-toluenesulfonyl chloride with triethylamine and 4-dimethylaminopyridine to give tosyl derivatives (**16**−**20**), which are the precursors of radiofluorination.

The radiosynthesis of [^{18}F]**1** ([^{18}F]Br-BIPF), [^{18}F]**2** ([^{18}F]Cl-BIPF), [^{18}F]**3** ([^{18}F]Me-BIPF), [^{18}F]**4** ([^{18}F]OMe-BIPF), and [^{18}F]**5** ([^{18}F]H-BIPF) was accomplished by nucleophilic displacement with a fluoride anion (Scheme 2). The radiochemical purities of all ^{18}F-labeled BIP derivatives were over 99%, with radiochemical yields of 37−65% (Figure S1 and Table S1). The molar activity of these compounds was greater than 8.4 MBq/mmol (Table S1). [^{18}F]RO-948, which is a second generation tau PET tracer (Figure S2), was synthesized with a slightly modified method from a previous report for use as a positive control tracer in this study.[16]

First, we carried out *in vitro* autoradiography (ARG) using AD brain sections to evaluate the selective binding affinity of ^{18}F-labeled BIP derivatives for tau aggregates. In the AD brain, amyloid-β (Aβ) aggregates often colocalize with tau aggregates.[2] Therefore, before performing *in vitro* ARG, the distribution of Aβ and tau aggregates in AD brain sections was confirmed by immunohistochemical staining with anti-Aβ and antiphosphorylated tau antibody (Figure S3). As shown in Figure 3, the radioactivity of all ^{18}F-labeled BIP derivatives was observed only in the gray matter of Aβ(+)/tau(+) brain sections. Similar to these compounds, we observed the radioactivity of [^{18}F]RO-948 only in the Aβ(+)/tau(+) brain section (Figure 3K and L). In addition, the pattern of radioactivity was consistent with the positive region of immunohistochemical staining with antiphosphorylated tau antibody. These results indicate that all ^{18}F-labeled BIP derivatives selectively bound to tau aggregates deposited on the AD brain sections. However, since this result is not quantitative, we performed a further study with AD brain sections to characterize of their binding affinity for tau aggregates.

In order to assess the effect of a substituted group or atom introduced into the 7-position of the BIP scaffold on the affinity for tau aggregates, an *in vitro* blocking study was carried out with [^{125}I]IBIPF1 as a competitive ligand. The radioactivity of [^{125}I]IBIPF1 in the gray matter was markedly decreased by adding nonradioactive BIP derivatives (Figure S4). Next, the region of interest (ROI) was set in the gray matter of the Aβ(+)/tau(+) brain section and the radioactivity accumulation (cpm/mm^2) was calculated (Figures S5 and S6). In the presence of BIP derivatives, the radioactivity of [^{125}I]IBIPF1 was reduced to 19−26% of the control, and these values were lower than in the presence of IBIPF1 (30%) (Figure 4). However, the difference in the blocking rate among

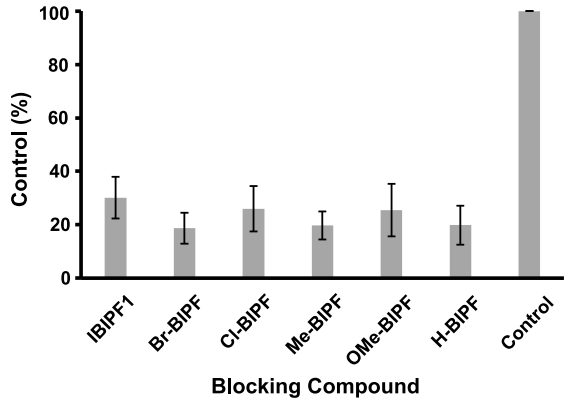

Figure 4. Binding rate of [^{125}I]IBIPF1 in AD brain sections after incubation with BIP derivatives.

BIP derivatives was not significant. The results of this study suggest that the substituted group or atom at the 7-position of the BIP scaffold does not makedly affect the binding affinity for tau aggregates. The results of structure−activity relationship studies in the past and the present study indicated that the 3-position of the BIP scaffold has a greater influence on the binding affinity with tau than the 7-position of the BIP scaffold.[14] On the other hand, these positions did not affect the affinity for Aβ aggregates. Because the structure of tau and Aβ aggregates deposited in the AD brain has yet to be fully elucidated, the binding site of the BIP scaffold remains unclear, but the 7-position of the BIP scaffold may be outside of the binding site in tau aggregates.

https://dx.doi.org/10.1021/acsmedchemlett.0c00641
ACS Med. Chem. Lett. 2021, 12, 262−266

Table 1. Brain Uptake of Radioactivity after the Injection of Each ^{18}F-Labeled BIP Derivative in Normal Mice[a] and the Ratio of Their Radioactivity Accumulation (2 min/60 min)

	% ID/g in the brain				ratio
compd	2 min	10 min	30 min	60 min	2 min/60 min
[^{18}F]Br-BIPF	6.29 (0.91)	2.64 (0.15)	1.81 (0.16)	1.92 (0.22)	3.28
[^{18}F]Cl-BIPF	6.38 (0.55)	2.86 (0.22)	2.31 (0.19)	2.16 (0.22)	2.95
[^{18}F]Me-BIPF	6.79 (0.83)	3.83 (0.51)	1.96 (0.17)	1.89 (0.11)	3.59
[^{18}F]OMe-BIPF	5.15 (0.20)	3.01 (0.33)	1.88 (0.33)	1.83 (0.17)	2.81
[^{18}F]H-BIPF	4.84 (0.44)	2.87 (0.07)	1.99 (0.20)	2.02 (0.21)	2.39
[^{18}F]IBIPF1[b]	6.22 (0.70)	3.68 (0.32)	2.77 (0.52)	2.01 (0.28)	3.09
[^{18}F]RO-948	4.16 (0.35)	1.36 (0.17)	0.24 (0.08)	0.13 (0.07)	32.0

[a]Each value represents the mean (SD) of five animals. [b]The data were reported previously.[15]

Next, a biodistribution study using normal mice was performed to evaluate uptake into and wash out from the brain after the injection of ^{18}F-labeled BIP derivatives (Tables 1 and S1). All compounds displayed high initial brain uptake at 2 min postinjection (4.84−6.79% ID/g). These values were higher than the criteria of the tau PET tracer (≥4% ID/g at 2 min postinjection in murine brain)[17,18] and [^{18}F]RO-948 (4.16% ID/g). Additionally, all ^{18}F-labeled BIP derivatives were washed out from the brain, but the 2 min/60 min ratios (2.40−3.59) were much lower than for [^{18}F]RO-948 (32.0). [^{18}F]Florbetapir, which is an Aβ imaging tracer for clinical use, also showed an almost equal 2 min/60 min ratio (3.80) to ^{18}F-labeled BIP derivatives under the same conditions.[19,20] Additionally, the brain uptake of all ^{18}F-labeled BIP derivatives at 2 min postinjection was higher than that of [^{18}F]Florbetapir (4.90% ID/g), suggesting that these compounds have favorable brain kinetics as a PET tracer. The brain uptake and 2 min/60 min ratio of [^{18}F]Br-BIPF and [^{18}F]Cl-BIPF were the same as for [^{18}F]IBIPF1, suggesting that the brain kinetics in the mouse do not depend on the type of halogen atom. On the other hand, the brain uptake of [^{18}F]Me-BIPF (6.79% ID/g), [^{18}F]OMe-BIPF (5.15% ID/g), and [^{18}F]H-BIPF (4.84% ID/g) at 2 min postinjection was different from [^{18}F]Br-BIPF (6.29% ID/g), [^{18}F]Cl-BIPF (6.38% ID/g), and [^{18}F]IBIPF1 (6.22% ID/g). Among the ^{18}F-labeled BIP derivatives, [^{18}F]Me-BIPF showed the highest brain uptake and 2 min/60 min ratio. These results reveal that the substituted group or atom at the 7-position of the BIP scaffold alters the brain kinetics. Compared with the BIP derivatives labeled with radioiodine, ^{18}F-labeled BIP probes developed in this study showed a lower 2 min/60 min ratio. Introduction of a fluoroethyl group is one of the typical methods for radiofluorination, but it may cause slow washout from major organs including the brain.[21,22] This may be one of the reasons for the difference. Therefore, varying the ^{18}F-labeled side chain including alkoxy group may improve the brain pharamacokinetics of ^{18}F-labeled BIP derivatives.

In conclusion, we newly designed and synthesized novel ^{18}F-labeled BIP derivatives as PET tracers targeting tau aggregates in the brain. The results revealed that all ^{18}F-labeled BIP derivatives selectively bound to tau aggregates in the AD brain sections. Additionally, the binding affinity for tau aggregates did not depend on the type of substituted group or atom introduced into the 7-position of the BIP scaffold. On the other hand, the 7-position of BIP scaffold affects the initial brain uptake in the mouse. Taken together, further optimization of the substituted group or atom at the 7-position of BIP scaffold to improve the brain kinetics may lead to the development of novel and useful tau PET tracers.

■ ASSOCIATED CONTENT

Supporting Information

The Supporting Information is available free of charge at https://pubs.acs.org/doi/10.1021/acsmedchemlett.0c00641.

Full experimental methods and results of immunohistochemical staining, *in vitro* autoradiography, and biodistribution study for all organs (PDF)

■ AUTHOR INFORMATION

Corresponding Authors

Hiroyuki Watanabe − *Department of Patho-Functional Bioanalysis, Graduate School of Pharmaceutical Sciences, Kyoto University, Kyoto 606-8501, Japan;* orcid.org/0000-0002-8873-1224; Phone: +81-75-753-4607; Email: hwatanabe@pharm.kyoto-u.ac.jp; Fax: +81-75-753-4568

Masahiro Ono − *Department of Patho-Functional Bioanalysis, Graduate School of Pharmaceutical Sciences, Kyoto University, Kyoto 606-8501, Japan;* orcid.org/0000-0002-2497-039X; Phone: +81-75-753-4556; Email: ono@pharm.kyoto-u.ac.jp; Fax: +81-75-753-4568

Authors

Yuta Tarumizu − *Department of Patho-Functional Bioanalysis, Graduate School of Pharmaceutical Sciences, Kyoto University, Kyoto 606-8501, Japan*

Sho Kaide − *Department of Patho-Functional Bioanalysis, Graduate School of Pharmaceutical Sciences, Kyoto University, Kyoto 606-8501, Japan*

Yoichi Shimizu − *Department of Patho-Functional Bioanalysis, Graduate School of Pharmaceutical Sciences, Kyoto University, Kyoto 606-8501, Japan; Department of Diagnostic Imaging and Nuclear Medicine, Graduate School of Medicine, Kyoto University, Kyoto 606-8507, Japan*

Shimpei Iikuni − *Department of Patho-Functional Bioanalysis, Graduate School of Pharmaceutical Sciences, Kyoto University, Kyoto 606-8501, Japan;* orcid.org/0000-0002-7073-9084

Yuji Nakamoto − *Department of Diagnostic Imaging and Nuclear Medicine, Graduate School of Medicine, Kyoto University, Kyoto 606-8507, Japan*

Complete contact information is available at: https://pubs.acs.org/10.1021/acsmedchemlett.0c00641

Notes

The authors declare no competing financial interest.

https://dx.doi.org/10.1021/acsmedchemlett.0c00641
ACS Med. Chem. Lett. 2021, 12, 262−266

■ ACKNOWLEDGMENTS

This research was supported by JSPS KAKENHI Grant Numbers JP17H05092 and JP17H05694 and The Mochida Memorial Foundation for Medical and Pharmaceutical Research. We thank Dr. Masafumi Ihara (National Cerebral and Cardiovascular Center) for providing brain samples of AD cases.

■ REFERENCES

(1) Invernizzi, G.; Papaleo, E.; Sabate, R.; Ventura, S. Protein aggregation: mechanisms and functional consequences. *Int. J. Biochem. Cell Biol.* **2012**, *44* (9), 1541−1554.
(2) Villemagne, V. L.; Fodero-Tavoletti, M. T.; Masters, C. L.; Rowe, C. C. Tau imaging: early progress and future directions. *Lancet Neurol.* **2015**, *14* (1), 114−124.
(3) Alzheimer's Association. 2017 Alzheimer's disease facts and figures. *Alzheimer's Dementia* **2017**, *13* (4), 325−373.
(4) Rajasekhar, K.; Govindaraju, T. Current progress, challenges and future prospects of diagnostic and therapeutic interventions in Alzheimer's disease. *RSC Adv.* **2018**, *8* (42), 23780−23804.
(5) Maruyama, M.; Shimada, H.; Suhara, T.; Shinotoh, H.; Ji, B.; Maeda, J.; Zhang, M. R.; Trojanowski, J. Q.; Lee, V. M.; Ono, M.; Masamoto, K.; Takano, H.; Sahara, N.; Iwata, N.; Okamura, N.; Furumoto, S.; Kudo, Y.; Chang, Q.; Saido, T. C.; Takashima, A.; Lewis, J.; Jang, M. K.; Aoki, I.; Ito, H.; Higuchi, M. Imaging of tau pathology in a tauopathy mouse model and in Alzheimer patients compared to normal controls. *Neuron* **2013**, *79* (6), 1094−1108.
(6) Harada, R.; Okamura, N.; Furumoto, S.; Furukawa, K.; Ishiki, A.; Tomita, N.; Tago, T.; Hiraoka, K.; Watanuki, S.; Shidahara, M.; Miyake, M.; Ishikawa, Y.; Matsuda, R.; Inami, A.; Yoshikawa, T.; Funaki, Y.; Iwata, R.; Tashiro, M.; Yanai, K.; Arai, H.; Kudo, Y. ^{18}F-THK5351: A Novel PET Radiotracer for Imaging Neurofibrillary Pathology in Alzheimer Disease. *J. Nucl. Med.* **2016**, *57* (2), 208−214.
(7) Leuzy, A.; Chiotis, K.; Lemoine, L.; Gillberg, P. G.; Almkvist, O.; Rodriguez-Vieitez, E.; Nordberg, A. Tau PET imaging in neurodegenerative tauopathies-still a challenge. *Mol. Psychiatry* **2019**, *24* (8), 1112−1134.
(8) Smith, R.; Wibom, M.; Pawlik, D.; Englund, E.; Hansson, O. Correlation of In Vivo [^{18}F]Flortaucipir With Postmortem Alzheimer Disease Tau Pathology. *JAMA Neurol* **2019**, *76* (3), 310−317.
(9) Betthauser, T. J.; Cody, K. A.; Zammit, M. D.; Murali, D.; Converse, A. K.; Barnhart, T. E.; Stone, C. K.; Rowley, H. A.; Johnson, S. C.; Christian, B. T. In Vivo Characterization and Quantification of Neurofibrillary Tau PET Radioligand ^{18}F-MK-6240 in Humans from Alzheimer Disease Dementia to Young Controls. *J. Nucl. Med.* **2019**, *60* (1), 93−99.
(10) Wong, D. F.; Comley, R. A.; Kuwabara, H.; Rosenberg, P. B.; Resnick, S. M.; Ostrowitzki, S.; Vozzi, C.; Boess, F.; Oh, E.; Lyketsos, C. G.; Honer, M.; Gobbi, L.; Klein, G.; George, N.; Gapasin, L.; Kitzmiller, K.; Roberts, J.; Sevigny, J.; Nandi, A.; Brasic, J.; Mishra, C.; Thambisetty, M.; Mogekar, A.; Mathur, A.; Albert, M.; Dannals, R. F.; Borroni, E. Characterization of 3 Novel Tau Radiopharmaceuticals, ^{11}C-RO-963, ^{11}C-RO-643, and ^{18}F-RO-948, in Healthy Controls and in Alzheimer Subjects. *J. Nucl. Med.* **2018**, *59* (12), 1869−1876.
(11) Kroth, H.; Oden, F.; Molette, J.; Schieferstein, H.; Capotosti, F.; Mueller, A.; Berndt, M.; Schmitt-Willich, H.; Darmency, V.; Gabellieri, E.; Boudou, C.; Juergens, T.; Varisco, Y.; Vokali, E.; Hickman, D. T.; Tamagnan, G.; Pfeifer, A.; Dinkelborg, L.; Muhs, A.; Stephens, A. Discovery and preclinical characterization of [^{18}F]PI-2620, a next-generation tau PET tracer for the assessment of tau pathology in Alzheimer's disease and other tauopathies. *Eur. J. Nucl. Med. Mol. Imaging* **2019**, *46* (10), 2178−2189.
(12) Sanabria Bohorquez, S.; Marik, J.; Ogasawara, A.; Tinianow, J. N.; Gill, H. S.; Barret, O.; Tamagnan, G.; Alagille, D.; Ayalon, G.; Manser, P.; Bengtsson, T.; Ward, M.; Williams, S. P.; Kerchner, G. A.; Seibyl, J. P.; Marek, K.; Weimer, R. M. [^{18}F]GTP1 (Genentech Tau Probe 1), a radioligand for detecting neurofibrillary tangle tau pathology in Alzheimer's disease. *Eur. J. Nucl. Med. Mol. Imaging* **2019**, *46* (10), 2077−2089.
(13) Ono, M.; Watanabe, H.; Kitada, A.; Matsumura, K.; Ihara, M.; Saji, H. Highly Selective Tau-SPECT Imaging Probes for Detection of Neurofibrillary Tangles in Alzheimer's Disease. *Sci. Rep.* **2016**, *6*, 34197.
(14) Kaide, S.; Ono, M.; Watanabe, H.; Kitada, A.; Yoshimura, M.; Shimizu, Y.; Ihara, M.; Saji, H. Structure-Activity Relationships of Radioiodinated Benzoimidazopyridine Derivatives for Detection of Tau Pathology. *ACS Med. Chem. Lett.* **2018**, *9* (5), 478−483.
(15) Kaide, S.; Watanabe, H.; Shimizu, Y.; Tatsumi, H.; Iikuni, S.; Nakamoto, Y.; Togashi, K.; Ihara, M.; Saji, H.; Ono, M. ^{18}F-labeled benzimidazopyridine derivatives for PET imaging of tau pathology in Alzheimer's disease. *Bioorg. Med. Chem.* **2019**, *27* (16), 3587−3594.
(16) Gobbi, L. C.; Knust, H.; Korner, M.; Honer, M.; Czech, C.; Belli, S.; Muri, D.; Edelmann, M. R.; Hartung, T.; Erbsmehl, I.; Grall-Ulsemer, S.; Koblet, A.; Rueher, M.; Steiner, S.; Ravert, H. T.; Mathews, W. B.; Holt, D. P.; Kuwabara, H.; Valentine, H.; Dannals, R. F.; Wong, D. F.; Borroni, E. Identification of Three Novel Radiotracers for Imaging Aggregated Tau in Alzheimer's Disease with Positron Emission Tomography. *J. Med. Chem.* **2017**, *60* (17), 7350−7370.
(17) Okamura, N.; Harada, R.; Furumoto, S.; Arai, H.; Yanai, K.; Kudo, Y. Tau PET imaging in Alzheimer's disease. *Curr. Neurol. Neurosci. Rep.* **2014**, *14* (11), 500.
(18) Harada, R.; Okamura, N.; Furumoto, S.; Yanai, K. Imaging Protein Misfolding in the Brain Using β-Sheet Ligands. *Front. Neurosci.* **2018**, *12*, 585.
(19) Yoshimura, M.; Ono, M.; Matsumura, K.; Watanabe, H.; Kimura, H.; Cui, M.; Nakamoto, Y.; Togashi, K.; Okamoto, Y.; Ihara, M.; Takahashi, R.; Saji, H. Structure-Activity Relationships and in Vivo Evaluation of Quinoxaline Derivatives for PET Imaging of β-Amyloid Plaques. *ACS Med. Chem. Lett.* **2013**, *4* (7), 596−600.
(20) Villemagne, V. L.; Dore, V.; Burnham, S. C.; Masters, C. L.; Rowe, C. C. Imaging tau and amyloid-β proteinopathies in Alzheimer disease and other conditions. *Nat. Rev. Neurol.* **2018**, *14* (4), 225−236.
(21) Watanabe, H.; Ono, M.; Kimura, H.; Kagawa, S.; Nishii, R.; Fuchigami, T.; Haratake, M.; Nakayama, M.; Saji, H. A dual fluorinated and iodinated radiotracer for PET and SPECT imaging of β-amyloid plaques in the brain. *Bioorg. Med. Chem. Lett.* **2011**, *21* (21), 6519−6522.
(22) Tago, T.; Furumoto, S.; Okamura, N.; Harada, R.; Adachi, H.; Ishikawa, Y.; Yanai, K.; Iwata, R.; Kudo, Y. Structure-Activity Relationship of 2-Arylquinolines as PET Imaging Tracers for Tau Pathology in Alzheimer Disease. *J. Nucl. Med.* **2016**, *57* (4), 608−614.

https://dx.doi.org/10.1021/acsmedchemlett.0c00641
ACS Med. Chem. Lett. 2021, 12, 262−266